How to Cite: Ivanova, N.M., Vissurkhanova, Ya.A., Soboleva, Ye.A., & Kenzhetaeva, S.O. (2024) Copper Nanoparticles Supported on Nickel Ferrite: Synthesis and Electrocatalytic Activity. *Eurasian Journal of Chemistry, 29, 3(115), 109–118.* https://doi.org/10.31489/2959-0663/3-24-2

Article

Received: 8 March 2024 | Revised: 30 June 2024 | Accepted: 19 July 2024 | Published online: 02 August 2024

UDC 544.653.3+546.56-121+544.478

https://doi.org/10.31489/2959-0663/3-24-2

Nina M. Ivanova[1*], Yakha A. Vissurkhanova[1,2], Yelena A. Soboleva[1], Saule O. Kenzhetaeva[2]

[1]*LLP "Institute of Organic Synthesis and Coal Chemistry of the Republic of Kazakhstan", Karaganda, Kazakhstan;*
[2]*Karaganda Buketov University, 28, Karaganda, Kazakhstan*
*(*Corresponding author's e-mail: nmiva@mail.ru)*

Copper Nanoparticles Supported on Nickel Ferrite: Synthesis and Electrocatalytic Activity

$Cu(x)/NiFe_2O_4(y)$ magnetic composites with different component ratios were prepared by chemical reduction of copper cations in the presence of sonicated nickel ferrite. Separately synthesized Cu and $NiFe_2O_4$ nanoparticles, as well as composites of copper particles supported on nickel ferrite, were characterized by X-ray diffraction spectroscopy and scanning electron microscopy. Based on the determination of the specific surface area, the $NiFe_2O_4$ sample heat-treated at 500 °C was selected as the support for the catalytically active Cu particles. The electrocatalytic activity of $Cu(x)/NiFe_2O_4(y)$ composites deposited on a cathode was investigated in the electrohydrogenation of acetophenone (APh). It was shown that the electrocatalytic activity of these composites appears starting from the percentage ratio of their components x:y = 40:60. This was expressed as an increase in the rate of electrocatalytic hydrogenation of APh and its conversion compared to the electrochemical reduction of APh under similar conditions. It was suggested that the slightly lower rate of APh hydrogenation on $Cu/NiFe_2O_4$ composites compared to Cu particles is due to the poor electrical conductivity of the nickel ferrite support.

Keywords: copper nanoparticles, chemical reduction, nickel ferrite carrier, co-precipitation method, catalysts, electrocatalytic hydrogenation, acetophenone, 1-phenylethanol.

Introduction

A significant advantage of magnetic catalysts over conventional "non-magnetic" catalysts is the ability to extract them from the reaction medium using a magnet with minimal loss of mass and activity. The use of magnetic catalysts ensures the high efficiency of catalytic reactions in general and contributes to their classification as processes that meet the basic postulates of "green chemistry" [1, 2].

Catalysts consisting of catalytically active mono- and bimetallic nanoparticles supported on magnetic carriers represent a distinct group among all magnetic catalysts that have attracted increased attention from researchers in the field of catalysis [1, 2]. Iron oxides are most commonly used as magnetic carriers, and the most studied is magnetite, Fe_3O_4. The demand for magnetite nanoparticles is determined by their magnetic properties, chemical stability, low toxicity, high specific surface area, cost-effectiveness, and relative ease of production [3, 4]. In this case, catalysts on Fe_3O_4 support are characterized by good reducibility and are widely used in various catalytic processes for environmental purification, as electrodes in electrocatalysis, in organic synthesis, drug delivery, cancer treatment, etc. [3–7].

Transition metal ferrites with magnetic properties are much less frequently used as supports for catalytically active particles than magnetite, and such studies have been described in the literature. For example, palladium nanoparticles supported on cobalt ferrite and zinc ferrite were shown to be effective in the ligand-free Suzuki coupling reaction [8, 9]. Catalysts consisting of Pd nanoparticles immobilized on nickel ferrite and magnetite modified with an amine were used for the hydrogenation of some of compounds with unsaturated C–C bonds, as well as nitro compounds and azides [10]. The catalytic activity of $NiFe_2O_4$@Cu nanoparticles was studied in the reduction reactions of nitroaromatic compounds using sodium borohydride, whose conversion to the corresponding amines was 30–100 %, depending on the structure of the starting nitroarenes [11]. Core-in-shell magnetic $NiFe_2O_4$@Au nanoparticles were prepared by gold reduction on the surface of nickel ferrite using the amino acid methionine as a reducing agent [12]. In [13], the structural and magnetic properties of composites of silver nanoparticles deposited on the surface of silica-coated nickel ferrite nanoparticles ($Ni_{1.43}Fe_{1.7}O_4$-SiO_2/Ag) were investigated.

The aim of this work is to prepare composites consisting of copper nanoparticles deposited on nickel ferrite and to study the possibility of using them as electrocatalysts in the model reaction of electrohydrogenation of acetophenone (APh). These studies were prompted by the need to find out the influence of the magnetic component — the carrier — on the electrocatalytic activity of copper nanoparticles in an electrolytic cell, on the outer side of which (under the cathode) there was a magnet holding the ferromagnetic catalyst in the form of powder on the cathode surface. This method was previously developed under the leadership of Professor I.V. Kirilyus using skeletal catalysts, which showed high electrocatalytic activity in the electrohydrogenation of many organic compounds [14–16]. Copper nanoparticles do not have magnetic properties and, when hydrogen is released at the cathode, they begin to periodically rise and fall back to the cathode surface, shortening the duration of their contact with the electrode, necessary to obtain a charge. This is thought to decrease their electrocatalytic activity. At the same time, copper particles show quite high activity in some processes of electrocatalytic hydrogenation of organic compounds comparable to magnetic nickel particles [17]. A detailed review of copper nanoparticles without and with deposition on supports of various nature (carbon materials, metal oxides, polymers, silica, oxides with a delafossite structure, etc.), as well as their use in catalytic reactions of organic transformations has been given in the recent paper [18].

Our previous research [19] found that nickel (II) ferrite, $NiFe_2O_4$, prepared by the co-precipitation method, unlike copper (II) ferrite [20], is not reduced in the electrochemical system and retains its stability in the alkaline medium of the catholyte, and does not show any catalytic effect in the electrohydrogenation reactions of organic compounds. Therefore, it can be used as a magnetic carrier for electrocatalytically active catalyst particles.

Experimental

Materials

Nickel nitrate $Ni(NO_3)_2 \cdot 6H_2O$, ferric nitrate ($Fe(NO_3)_3 \cdot 9H_2O$), sodium hydroxide (NaOH), copper nitrate ($Cu(NO_3)_2 \cdot 3H_2O$), hydrazine hydrate (N_2H_5OH, 64 %) and ethylene glycol ($C_2H_6O_2$, analytical grade) were purchased from "Ridder" LLP (Karaganda, Kazakhstan) and used without further purification. Polyvinyl alcohol (PVA) (Mw = 9,000–10,000 $g \cdot mol^{-1}$) and polyvinylpyrrolidone (PVP) (Mw = 10,000 $g \cdot mol^{-1}$) were purchased from Sigma-Aldrich. Distilled water and medical grade ethyl alcohol (96 %) were used to prepare the required solutions and wash the prepared particles.

Nickel (II) Ferrite Preparation

Nickel (II) ferrite ($NiFe_2O_4$) was synthesized by the co-precipitation method according to the procedure described in [18]. Nickel nitrate (0.06 mol) and ferric nitrate (0.12 mol) were dissolved in 300 ml of distilled water. Then, a 2M NaOH solution was added to pH = 12. The resulting mixture was stirred at 40 °C for 1 h. It was filtered and washed thoroughly with hot distilled water to pH 7. The precipitate was dried at 80 °C. Equal amounts of the resulting powder were thermally treated at 500 °C and 700 °C for 2 h under conditions with limited oxygen access (in crucibles with closed lids). The powders were then ground in an electric mill.

Synthesis of Cu Nanoparticles

Copper (II) nitrate (0.025 mol) was dissolved in a solution of 200 ml of ethylene glycol and 200 ml of distilled water. An aqueous solution of 1 M NaOH was then slowly added to the reaction mixture until pH = 12. Subsequently, hydrazine hydrate (1 mol) was added dropwise. The reaction mixture was kept at 60 °C for 1 h. During the vigorous reaction, the formation of red-brown copper particles was observed. The resulting Cu particles were separated by centrifugation, washed with 100 ml of distilled water and ethyl alcohol heated to 30 °C. Then, they were dried under vacuum at 80 °C. Cu nanoparticles were also prepared using a similar procedure with the reduction of the metal salt in the presence of polymer particle stabilizers (PVA and PVP).

Synthesis of Cu(x)/$NiFe_2O_4$(y) Composites

Ethylene glycol (200 ml) was added to the selected amount of $NiFe_2O_4$ (500 °C). The mixture was subjected to ultrasonic treatment for 30 minutes. Then, 200 ml of an aqueous solution containing the required amount of copper nitrate was added and stirred for 30 min. The pH was then adjusted to 12 using 1 M NaOH solution. The required amount of hydrazine hydrate was then added dropwise to reduce copper, keeping the molar ratio $Cu(NO_3)_2/N_2H_4$ = 1:40. The reaction mixture was kept at a temperature of 60 °C. The resulting particles were separated by centrifugation and washed with distilled water and ethyl alcohol heated to 30 °C. Then, they were dried under vacuum at 80 °C to a constant weight. Thus, Cu(x)/$NiFe_2O_4$(y) composites were

obtained with different percentage ratios of copper to nickel ferrite: *x*:*y* = 80:20; 70:30; 60:40; 50:50; 40:60; 30:70; 20:80. The Cu(50)/ $NiFe_2O_4$ (50) + PVA/PVP composites were also prepared by adding copper nitrate to a 3 % polymer (PVA or PVP) aqueous solution and subsequent reduction using the similar procedure.

The metal content in the filtrates after the synthesis of nickel ferrite and Cu(*x*)/$NiFe_2O_4$(*y*) composites was determined by selective complexometric titration methods [17, 21]. Based on the titration results, it was established that there were no copper and nickel cations in the resulting transparent filtrates.

Study of the Electrocatalytic Activity of Cu(x)/$NiFe_2O_4$(y) Composites

The electrocatalytic activity of the obtained supported Cu(*x*)/$NiFe_2O_4$(*y*) composites as catalysts was studied in the electrohydrogenation of an aromatic ketone, acetophenone: C_6H_5–C(O)–CH_3 → C_6H_5–CH(OH)–CH_3. The experiments were carried out in a diaphragm electrochemical cell in an aqueous-alkaline solution (the initial NaOH concentration was 2 %) at a current of 2.5 A and a temperature of 30 °C. The powder of the prepared catalysts weighing 1 g was deposited on a horizontally located copper cathode (with an area of 0.09 dm^2) tightly adjacent to the bottom of the electrolytic cell. The catalysts with magnetic properties were held on the cathode by an external magnet placed outside the electrolyzer. The magnetic induction of the magnetic field generated was 0.05 T. A platinum grid served as the anode. Electrocatalytic hydrogenation of APh (with an initial concentration in the catholyte of 0.137 mol/L) was also carried out in an aqueous-alkaline solution of the catholyte at a current of 2.5 A, and a temperature of 30 °C.

Characterization

The structural phase characteristics of the synthesized nickel ferrite and composites of copper particles deposited on nickel ferrite were studied on a D8 ADVANCE ECO diffractometer (Bruker, Germany) using CuKα radiation in the angular range (2θ) 15–90°. The morphological characteristics of heat-treated samples of nickel ferrites and Cu(*x*)/$NiFe_2O_4$(*y*) composites were studied on a TESCAN MIRA 3 scanning electron microscope (SEM) (Czech Republic) using secondary (SE) and backscattered (BSE) electron detectors. The samples were analyzed with a conductive carbon layer deposited on them. Elemental microanalysis of the composites was performed using an X-Act energy dispersive detector (Oxford Instruments). Photographs of the deposited Cu catalyst particles were taken on a Levenhuk DTX 90 digital USB microscope (Russia). The specific surface area (SSA) of nickel ferrite particles was determined from nitrogen adsorption data obtained on a Sorbi-MS instrument (Russia) using the BET (Brunauer, Emmett and Teller) method, and the pore size distributions were established using the statistical thickness surface area (STSA) method.

Results and Discussion

According to the XRD analyses, the composition of the copper nanoparticles reduced separately by hydrazine hydrate in a water + EG medium contains, in addition to the crystalline phases of copper, oxides copper (CuO, Cu_2O) phases (Fig. 1, a). The content of these phases in the sample after synthesis is as follows: 81.6 % Cu, 9.4 % Cu_2O, and 9.0 % CuO. After electrochemical experiments, the copper and Cu_2O contents in the composition of these particles increase to 88.2 % and 11.8 %, respectively, while the CuO phases disappear (Fig. 1, b). Obviously, in the electrochemical system, copper cations are reduced from CuO oxide with the formation of copper in the zero-valent state, and Cu_2O is additionally formed. The size of Cu particles after synthesis, calculated using diffractometer software, is 44 nm (for the crystalline phase (111) at an angle of 2θ = 43.03°), and increases to 52 nm after the electrochemical experiments.

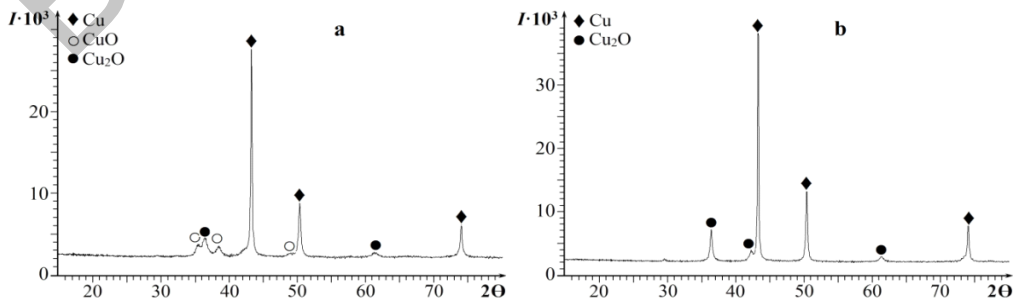

Figure 1. XRD patterns of Cu nanoparticles before (*a*) and after (*b*) electrohydrogenation of APh

Micrographs of the synthesized Cu particles (Fig. 2) show that they have the shape of short nanorods or nanotubes (~30–60 nm in diameter), some of which are pointed. These nanorods assemble chaotically into spiny little balls ("hedgehogs") of different sizes (~100–500 nm) forming a loose mass. An elemental analysis by energy dispersive X-ray spectroscopy (EDS) (spectrum 2) shows the presence of Cu with a small amount of oxygen. It is interesting to note that when the synthesis of copper nanoparticles is carried out only in an aqueous medium without a stabilizer, and hydrazine hydrate is also used for the reduction, then the particles have a layered structure with an approximately round shape and sizes of 100–400 nm [22]. The use of stabilizers such as PVP, polyethylene glycol, and starch contributes to a decrease in the size of copper nanoparticles to 70–100, 30–50 and 50–70 nm, respectively.

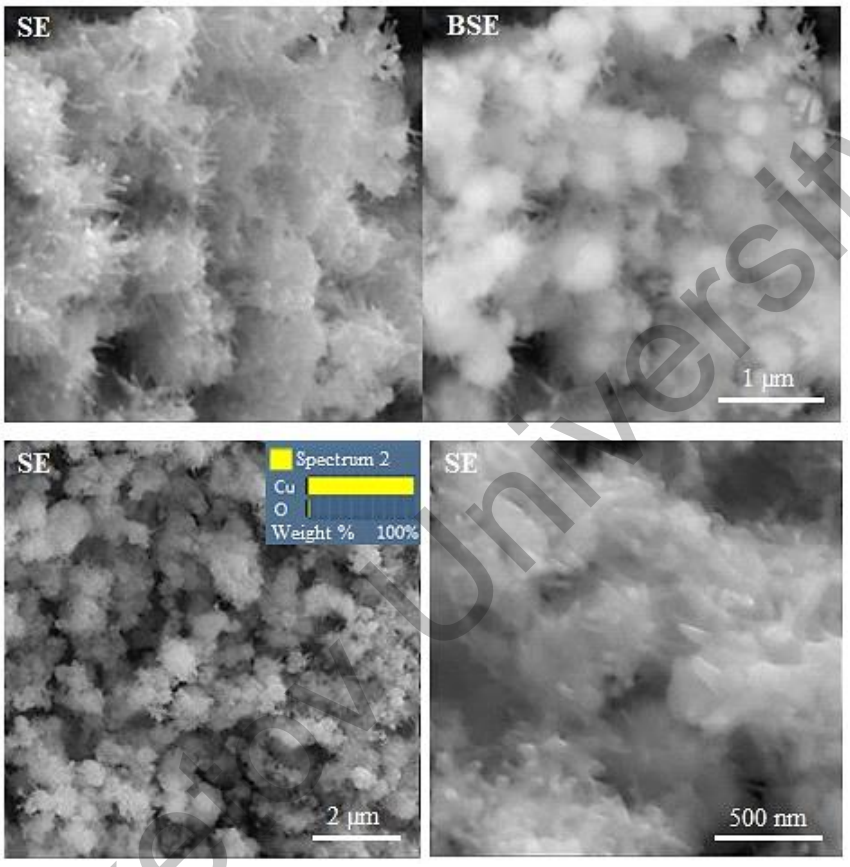

Figure 2. SEM images of Cu nanoparticles after synthesis in different scanning scales

Nickel (II) ferrite was prepared by the co-precipitation method followed by heat treatment at 500 °C and 700 °C. The phase composition of both heat-treated samples is represented by crystalline phases of nickel ferrite $NiFe_2O_4$ of cubic structure and hematite phases (α-Fe_2O_3) in small quantities (Fig. 3). The particle sizes in these nickel ferrite samples, according to the X-ray diffraction data, are 14 and 25 nm (for the (311) phase at a diffraction angle of 2θ = 35.7–35.6°), i.e. the size of the nickel ferrite nanoparticles increases with increasing temperature.

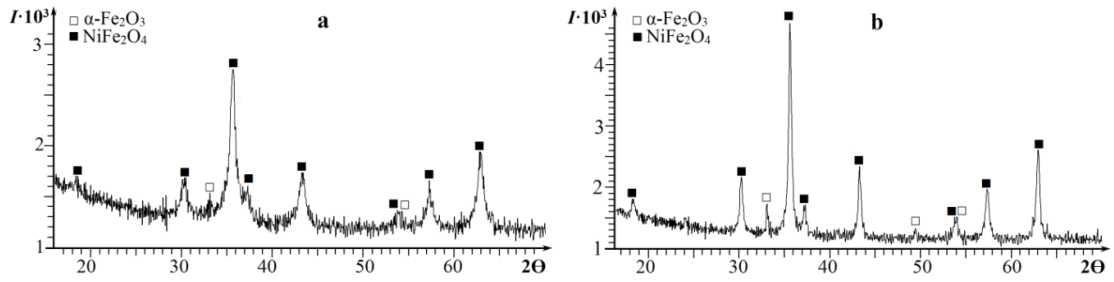

Figure 3. XRD patterns of $NiFe_2O_4$ (500 °C) (*a*) and $NiFe_2O_4$ (700 °C) (*b*) samples

Micrographs of nickel ferrite (Fig. 4) show that the particles in both samples are round in shape and vary slightly in size (~35–80 nm). At the same time, the somewhat amorphous particles of the $NiFe_2O_4$ (500 °C) sample are pressed together more tightly than the particles of the $NiFe_2O_4$ (700 °C) sample, which are grouped into cluster structures resembling a torus (donut) shape. Both nickel ferrite samples have magnetic properties, confirming magnetism studies carried out on nickel ferrite nanoparticles fabricated under similar conditions by the co-precipitation method [23]. For example, for $NiFe_2O_4$ nanoparticles with an average size of 28 nm, the saturation magnetization (M_S) at room temperature was ~40.5 emu/g, which is lower than that of a bulk sample of this ferrite (56 emu/g). For comparison, the M_S value for magnetite (Fe_3O_4) nanoparticles with sizes of ~20 nm at room temperature is 75.3 emu/g [24]. The given M_S values show that the magnetic properties of nickel ferrite are somewhat weaker than those of magnetite.

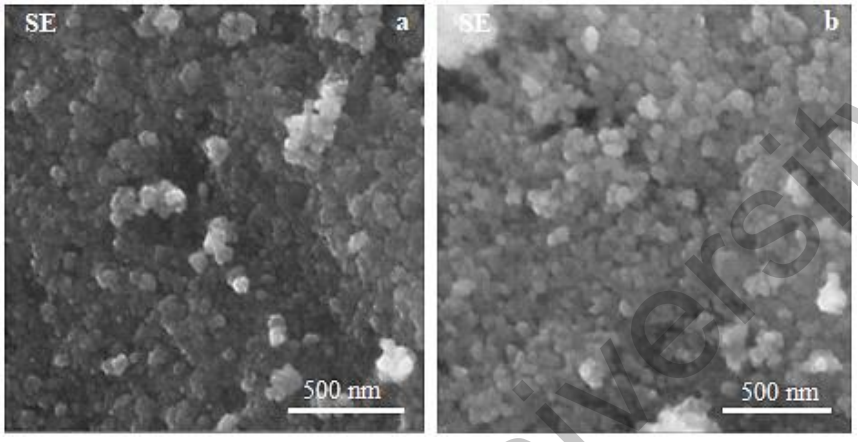

Figure 4. SEM images of $NiFe_2O_4$ (500 °C) (*a*) and $NiFe_2O_4$ (700 °C) (*b*)

In order to select one of the two nickel ferrite samples as a carrier for catalytically active copper nanoparticles, their specific surface area (SSA) was measured using the nitrogen adsorption-desorption isotherm in the BET method following the STSA calculations for the pore size distribution (Table 1).

Table 1

Specific surface area and porosity data for $NiFe_2O_4$ samples

Nickel ferrite sample	SSA, m^2/g	$V_{\Sigma\ pores}$, cm^3/g	Pore size distribution, %	
			mesopores	macropores
$NiFe_2O_4$ (500 °C)	72.7±1.4	0.135	45.0	55.0
$NiFe_2O_4$ (700 °C)	22.8±0.4	0.069	32.3	67.7

It is known that in solid materials, including powders, the pores present are classified according to their size into micropores (< 2 nm), mesopores (2–50 nm) and macropores (> 50 nm) [25]. In the both samples, the average pore sizes are 3–15, 56 and 80 nm, but with different volume ratios. According to Table 1, the total pore volume in the $NiFe_2O_4$ (500 °C) sample is larger than in the $NiFe_2O_4$ sample treated at 700 °C. Moreover, in the second sample, the volume of macropores relative to the total pore volume ($V_{\Sigma\ pores}$) exceeds the volume of mesopores by more than two times, which is apparently due to a greater degree of particle aggregation in this sample and the larger sizes of the aggregates formed. The specific surface area of particles in the $NiFe_2O_4$ (500 °C) sample is also significantly larger than in the $NiFe_2O_4$ (700 °C) sample. Since the best values for supporting catalyst particles are higher values of these structural characteristics, the nickel ferrite sample with heat treatment at 500 °C was chosen to create catalytic systems with supported copper particles.

Syntheses of supported Cu(*x*)/$NiFe_2O_4$ (500 °C)(*y*) composites were carried out with different ratios of copper particles and nickel ferrite (see synthesis procedure). Figure 5 shows the X-ray diffraction patterns for the Cu(50)/$NiFe_2O_4$(50) sample after synthesis and after electrocatalytic hydrogenation of acetophenone.

In the XRD patterns of the Cu(50)/$NiFe_2O_4$(50) sample, the intensity of the peaks of the crystalline phases of copper is significantly higher than the intensity of the nickel ferrite peaks, which corresponds to their values in the XRD patterns of individual components (Figures 1 and 3). In the constitution of this com-

posite after its use as a catalyst in the electrohydrogenation of APh, the crystalline phases of copper and nickel ferrite remain and the phases of copper (I) oxide appear in small amounts (Figure 5, *b*).

Micrographs of the synthesized Cu(50)/$NiFe_2O_4$(50) composite (Figure 6, *a*) show that copper particles in the form of rounded formations of different sizes (~100–800 nm) (highlighted in white) are located on the surface of nickel ferrite and some of them are also found among the nickel ferrite particles. There are also separate clusters of round copper particles connected to each other.

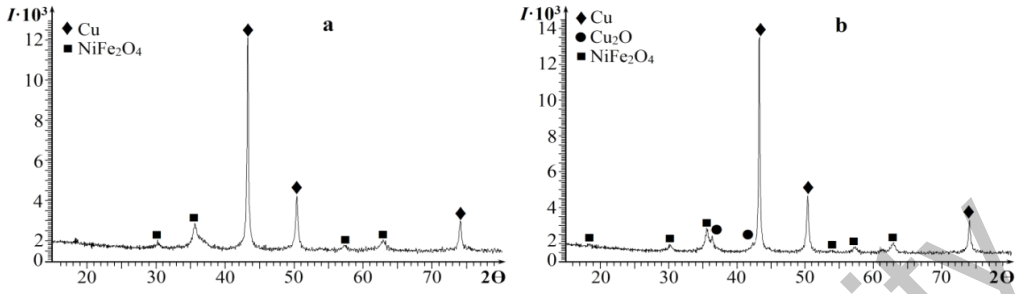

Figure 5. XRD patterns of Cu(50)/$NiFe_2O_4$(50) sample after synthesis (*a*) and after electrocatalytic hydrogenation of APh (*b*)

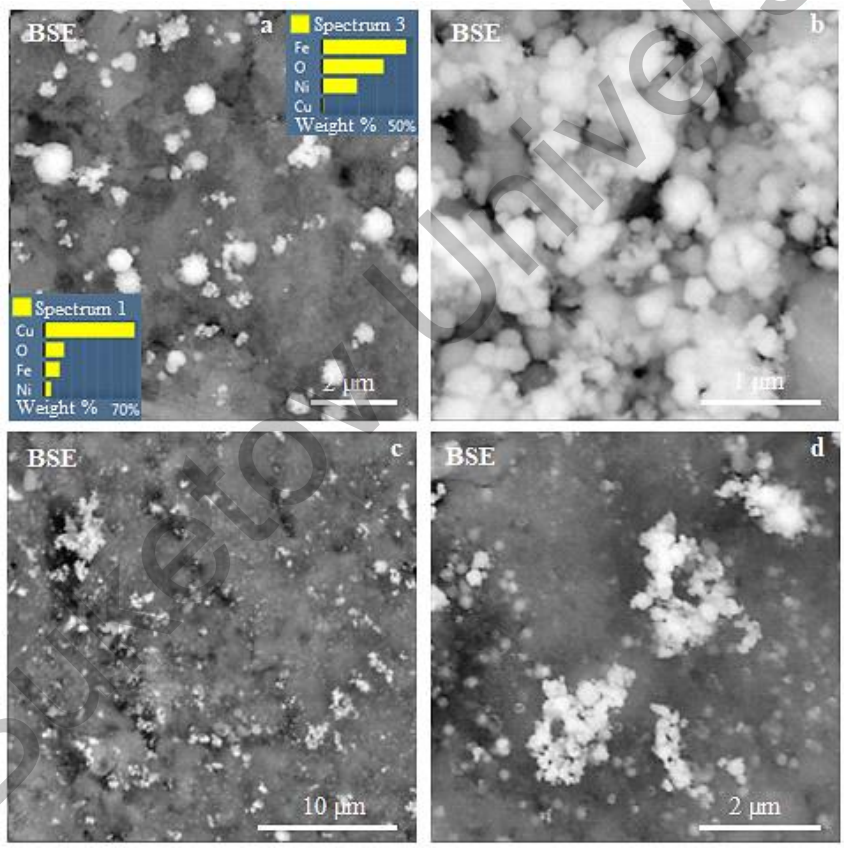

Figure 6. SEM images of Cu(50)/$NiFe_2O_4$(50) composite after synthesis (*a*, *b*) and after electrocatalytic hydrogenation of APh (*c*, *d*)

The shape of the copper particles in the Cu(50)/$NiFe_2O_4$(50) composite differs from the copper balls consisting of nanorods in the case of individual reduction under the same conditions (Fig. 2). It is possible that during the synthesis of the composite, small particles of nickel ferrite serve as initial grains for the formation of copper particles, which then take a rounded shape to form core-in-shell particles. After electrocatalytic application, the structure of this catalyst remains practically unchanged (Fig. 6, *c* and *d*).

The presence of magnetic properties in the synthesized Cu(50)/$NiFe_2O_4$(50) composite is demonstrated by the photographs in Figure 7. Without applying a magnet (Fig. 7, *a*), all particles simply lie on the glass surface and are visible as particles with a metallic sheen — these are obviously nickel ferrite and red-brown

particles of copper itself and copper on the support. In the presence of a magnet (Fig. 7, *b*), all particles are arranged in the form of fir trees perpendicular to the surface.

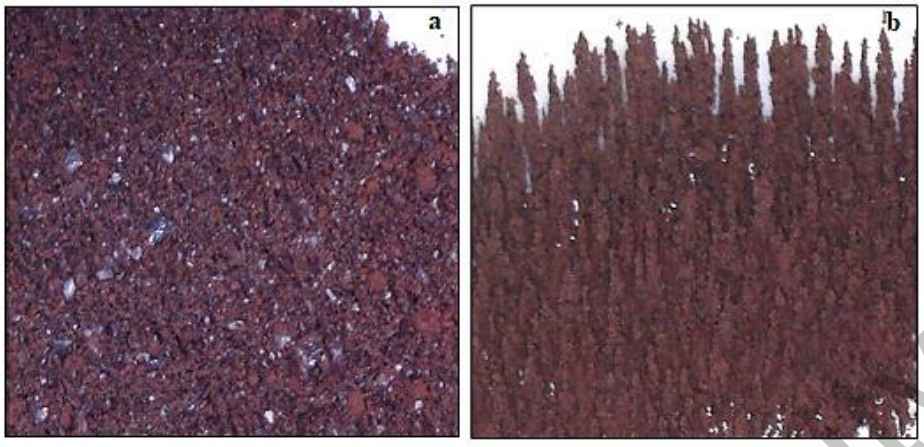

Figure 7. Photographs of Cu(50)/$NiFe_2O_4$(50) composite without (*a*) and with magnet (*b*)

All synthesized Cu(*x*)/$NiFe_2O_4$(500 °C)(*y*) composites with different percentages ratios of copper particles and carrier were deposited on the surface of a copper cathode, on the outer side of which a magnet was placed, in a diaphragm cell in an aqueous-alkaline catholyte solution. As the measurements of the gases released (hydrogen and oxygen) showed, the electrolysis of a NaOH aqueous solution was accompanied by an additional release of oxygen (V_{O_2} values in Table 2).

Table 2

Results of electrocatalytic hydrogenation of acetophenone on Cu particles and Cu/$NiFe_2O_4$ catalysts

Catalyst	Copper content in 1 g of catalyst, g	Electrochemical reduction of copper oxides		Electrocatalytic hydrogenation of acetophenone				
		τ, min	V_{O_2}, ml	*W*, ml H_2/min (α = 0.25)	η, %	α, %	Composition of extracts, %	
							1-PhE	APh
Cu cathode	–	–	0.0	9.6	56.7	95.5	90.80	4.93
Cu (0.5 g)	0.47	30	47.7	13.5	77.5	99.0	99.78	0.22
Cu + PVA (0.5 g)	0.49	20	31.2	13.4	75.0	100.0	99.77	0.23
Cu + PVP (0.5 g)	0.49	20	31.0	13.3	75.0	100.0	99.83	0.17
Cu(20) / $NiFe_2O_4$(80)	0.20	30	21.2	7.6	45.0	99.8	99.76	0.24
Cu(30) / $NiFe_2O_4$(70)	0.30	40	29.7	7.8	45.8	100.0	99.54	0.46
Cu(40) / $NiFe_2O_4$(60)	0.40	30	28.8	10.5	60.0	100.0	99.85	0.15
Cu(50) / $NiFe_2O_4$(50)	0.51	30	26.0	11.5	66.3	100.0	99.82	0.18
Cu(50)/$NiFe_2O_4$(50) + PVA	0.49	20	35.3	10.6	60.0	100.0	99.75	0.25
Cu(50)/$NiFe_2O_4$(50) + PVP	0.49	20	35.3	11.1	62.5	100.0	99.23	0.77
Cu(60) / $NiFe_2O_4$(40)	0.60	30	25.4	12.3	72.5	100.0	99.86	0.14
Cu(70) / $NiFe_2O_4$(30)	0.69	30	55.5	12.4	72.5	100.0	99.89	0.11
Cu(80) / $NiFe_2O_4$(20)	0.79	30	55.5	12.4	72.5	100.0	99.88	0.12
$NiFe_2O_4$ (500 °C)	–	0	0.0	–	–	–	–	–
$NiFe_2O_4$ (700 °C)	–	0	0.0	–	–	–	–	–

This indicates the occurrence of electrochemical reduction of copper cations from its existing oxides in the composites deposited on the cathode:

Cu cathode: $CuO + 2e^- + H_2O \rightarrow Cu^0 + 2OH^-$

$2H_2O + 2e^- \rightarrow H_2 + 2OH^-$

Pt anode: $4OH^- \rightarrow O_2 + 2H_2O + 4e^-$

The V_{O_2} values given in Table 2 can be used to assess the content of copper oxides in the composition of copper particles deposited on nickel ferrite. These data indicate that copper oxides are present in almost all copper particles reduced in the presence of a carrier, polymer particle stabilizers and without any additives to the reaction medium of their synthesis (Table 2). Perhaps partial oxidation of copper occurs when its particles are washed after synthesis and dried.

After completion of the electrochemical reduction of copper oxides (when the release of additional volumes of oxygen was terminated), an organic substance was introduced into the catholyte to carry out its electrocatalytic hydrogenation in the presence of Cu(*x*)/$NiFe_2O_4$(500 °C)(*y*) catalysts held on the cathode by an external magnet. The results obtained are presented in Table 2, which lists such characteristics as: V_{O_2} is the volume of additionally released oxygen as a result of the electrochemical reduction of copper oxides contained in its particles; τ is the process duration; *W* is the average rate of APh hydrogenation over a period equal to $\alpha = 0.25$; η is the hydrogen utilization coefficient at the same value of α, and α is the APh conversion. The same Table shows that samples of nickel ferrite with heat treatment at 500 and 700 °C are not reduced in the electrochemical system under the given conditions and do not exhibit electrocatalytic activity in the electrohydrogenation of acetophenone.

For comparison, Table 2 shows the results of the electrochemical reduction of APh on a Cu cathode (without a catalyst) and its electrocatalytic hydrogenation on copper nanoparticles synthesized without and in the presence of polymer stabilizers. These data show that the rate of electrochemical reduction of APh under the given conditions is quite high (9.6 ml H_2/min), but the process does not proceed to completion and with the formation of a small amount of by-products. The electrocatalytic hydrogenation of APh on copper particles and on Cu(*x*)/$NiFe_2O_4$(*y*) supported catalysts was carried out almost completely and without by-products, which was confirmed by chromatographic analyzes (Table 2). At the same time, the highest rates of APh hydrogenation were observed in processes using Cu particles (13.3–13.5 ml H_2/min).

For processes on supported catalysts, the rate of hydrogenation depends on the content of copper particles in their composition: the more there are, the higher is the rate of APh hydrogenation, and starting from the ratio *x*:*y* = 60:40 it almost does not change. Therefore, this percentage ratio of copper particles to nickel ferrite can be considered as optimal for this catalyst. However, it should be noted that the rate of APh hydrogenation on catalysts with the particle content $x > 60$ % is lower than that on copper nanoparticles (Table 2). It can be assumed that nickel ferrite, which has poor electrical conductivity, slows down the transfer of charge from the cathode to catalytically active copper particles, which is also reflected in the rate of electrocatalytic hydrogenation of the organic compound. In general, Cu(*x*)/$NiFe_2O_4$(*y*) supported catalysts, starting from the ratio *x*:*y* = 40:60, exhibit electrocatalytic activity in the studied process of electrohydrogenation of acetophenone with the selective formation of 1-phenylethanol, a fragrant substance with the hyacinth odor.

Conclusions

Magnetic composites of Cu nanoparticles supported on nickel ferrite with different contents of their components were synthesized by the reduction of copper cations in the presence of $NiFe_2O_4$ prepared by the co-precipitation procedure. Their structure, morphological features, and electrocatalytic properties in the electrohydrogenation of acetophenone were studied. It was found that the electrocatalytic activity of the resulting composites was manifested in the process studied starting from the Cu(40 %):$NiFe_2O_4$(60 %) ratio. The rate of APh electrohydrogenation increases compared to its electrochemical reduction on a copper cathode (without a catalyst). Its conversion with the selective formation of 1-phenylethanol reaches maximum values. It was suggested that the slightly lower rate of APh electrohydrogenation on Cu/$NiFe_2O_4$ composite-catalysts compared to Cu particles is due to the known poor electrical conductivity of nickel ferrite, which slows down the charge transfer from the cathode to the catalytically active copper particles.

Funding

This research was funded by the Science Committee of the Ministry of Science and Higher Education of the Republic of Kazakhstan (Program No. BR24992921).

*Author Information**

**The authors' names are presented in the following order: First Name, Middle Name and Last Name*

Nina Mikhailovna Ivanova (*corresponding author*) — Doctor of Chemical Sciences, Full Professor, Head of the Laboratory of Electrocatalysis and Quantum-chemical Research, LLP "Institute of Organic Syn-

thesis and Coal Chemistry of the Republic of Kazakhstan", Alikhanov Street, 1, 100000, Karaganda, Kazakhstan; e-mail: nmiva@mail.ru; https://orcid.org/0000-0001-8564-8006

Yakha Amkhadovna Vissurkhanova — Researcher, Laboratory of Electrocatalysis and Quantum-chemical Research, LLP "Institute of Organic Synthesis and Coal Chemistry of the Republic of Kazakhstan", Alikhanov Street, 1, 100000, Karaganda, Kazakhstan; Teacher, Department of Physical and Analytical Chemistry, Karaganda Buketov University, Universitetskaya street, 28, 100024, Karaganda, Kazakhstan; e-mail: yakhavisurkhanova@bk.ru; https://orcid.org/0000-0001-7279-1145

Yelena Anatol'evna Soboleva — Candidate of Chemical Sciences, Leading researcher, Laboratory of Electrocatalysis and Quantum-chemical Research, LLP "Institute of Organic Synthesis and Coal Chemistry of the Republic of Kazakhstan", Alikhanov Street, 1, 100000, Karaganda, Kazakhstan; e-mail: esoboleva-kz@mail.ru; https://orcid.org/0000-0002-1089-367X

Saule Orynbaevna Kenzhetaeva — Candidate of Chemical Sciences, Professor, Department of Organic Chemistry and Polymers, Karaganda Buketov University, Universitetskaya street, 28, 100024, Karaganda, Kazakhstan; e-mail: kenzhetaeva58@mail.ru; https://orcid.org/0000-0003-1891-5236

Author Contributions

The manuscript was written through contributions of all authors. All authors have given approval to the final version of the manuscript. CRediT: **Nina Mikhailovna Ivanova** conceptualization, writing-original draft, methodology, validation, visualization, funding acquisition, writing-review & editing; **Yakha Amkhadovna Vissurkhanova** investigation, methodology, data curation, Figures design, visualization; **Yelena Anatol'evna Soboleva** investigation, data curation, resources, visualization; **Saule Orynbaevna Kenzhetaeva**, investigation, data curation, formal analysis, validation.

Conflicts of Interest

The authors declare no conflict of interest.

References

1 Rossi, L.M., Costa, N.J.S., Silva, F.P., & Goncalves, R.V. (2013). Magnetic nanocatalysts: supported metal nanoparticles for catalytic applications. *Nanotechnol. Rev.*, *2*(5), 597–614. https://doi.org/10.1515/ntrev-2013-0021

2 Rossi, L.M., Ferraz, C.P., Fiorio, J.L., & Vono, L.L.R. (2021). Magnetically Recoverable Nanoparticle Catalysts. *Nanoparticles in Catalysis*, 159–181. Portico. https://doi.org/10.1002/9783527821761.ch8

3 Wu, W., Wu, Z., Yu, T., Jiang, C., & Kim, W.-S. (2015). Recent progress on magnetic iron oxide nanoparticles: synthesis, surface functional strategies and biomedical applications. *Sci. Technol. Adv. Mater.*, *16*, 023501, 43. https://doi.org/10.1088/1468-6996/16/2/023501

4 Liu, M., Ye, Y., Ye, J., Gao, T., Wang, D., Chen, G., & Song, Z. (2023). Recent advances of magnetite (Fe_3O_4)-based magnetic materials in catalytic applications. *Magnetochem.*, *9*(4), 110. https://doi.org/10.3390/magnetochemistry9040110

5 Pham, V.L., Kim, D.-G., & Ko,S.-O. (2018). Oxidative degradation of the antibiotic oxytetracycline by Cu@Fe_3O_4 core-shell nanoparticles. *Science of the Total Environment*., *631-632*, 608–618. https://doi.org/10.1016/j.scitotenv.2018.03.067

6 Zhao, Z., Cai, Z., Yang, L., Hu, Z., Zhang, Y., Peng, X., Wang, Q., Yuan, X., & Li, G. (2018). Ternary magnetic Ag–Cu/Fe_3O_4/rGO composite as an efficient photocatalyst for degradation of malachite green. *J. Mater. Sci: Mater. Electron*., *29*, 17743–17749. https://doi.org/10.1007/s10854-018-9881-7

7 Zhang, Y., Yan, W., Sun, Z., Li, X., & Gao, J. (2014). Fabrication of magnetically recyclable Ag/Cu@Fe_3O_4 nanoparticles with excellent catalytic activity for *p*-nitrophenol reduction. *RSC Advances*, *4*(72), 38040–38047. https://doi.org/ HYPERLINK "http://dx.doi.org/10.1039/C4RA05514D"10.1039/C4RA05514D

8 Senapati, K.K., Roy, S., Borgohain, C., & Phukan, P. (2012). Palladium nanoparticle supported on cobalt ferrite: An efficient magnetically separable catalyst for ligand free Suzuki coupling. *J. Mol. Catal. A: Chem.*, *352*, 128–134. https://doi.org/10.1016/j.molcata.2011.10.022

9 Singh, A.S., Patil, U.B., & Nagarkar, J.M. (2013). Palladium supported on zinc ferrite: A highly active, magnetically separable catalyst for ligand free Suzuki and Herck coupling. *Catal. Commun.*, *35*, 11–16. https://doi.org/10.1016/j.catcom.2013.02.003

10 Guin, D., Baruwati, B., & Manorama, S.V. (2007). Pd on amine-terminated ferrite nanoparticles: A complete magnetically recoverable facile catalyst for hydrogenation reactions. *Organic Letters*, *9*(7), 1419–1421. https://doi.org/10.1021/ol070290p

11 Zeynizadeh, B., Mohammadzadeh, I., Shokri, Z., & Hosseini, S.A. (2017). Synthesis and characterization of $NiFe_2O_4$@Cu nanoparticles as a magnetically recoverable catalyst for reduction of nitroarenes to arylamines with $NaBH_4$. *J. Colloid. Interface Sci.*, 500, 285–293. https://doi.org/10.1016/j.jcis.2017.03.030

12 Saykova, D., Saikova, S., Mikhlin, Yu., Panteleeva, M., Ivantsov, R., & Belova, E. (2020). Synthesis and characterization of core-shell magnetic nanoparticles $NiFe_2O_4$@Au. *Metals*, *10*(8), 1075. https://doi.org/ HYPERLINK "https://doi.org/%2010.3390/met10081075" HYPERLINK "https://doi.org/%2010.3390/met10081075"10.3390/met10081075

13 Blanco-Esqueda, I. G., Ortega-Zarzosa, G., Martínez, J. R., & Guerrero, A. L. (2015). Preparation and Characterization of Nickel Ferrite-SiO_2/Ag Core/Shell Nanocomposites. *Advances in Materials Science and Engineering, 2015*, 1–7. https://doi.org/10.1155/2015/678739

14 Kirilyus, I.V. (1981). *Elektrokataliticheskoe gidrirovanie [Electrocatalytic hydrogenation]*. Alma-Ata: Nauka KazSSR [in Russian].

15 Kirilyus, I.V., Muldakhmetov, M.Z., Filimonova, V.I., & Bekenova, U.B (1997). *Elektrokataliticheskoe gidrirovanie atsetilenovykh spirtov [Electrocatalytic hydrogenation of acetylene alcohols]*. Almaty: «Gylym» [in Russian].

16 Ivanova, N.M., Soboleva, Ye.A., & Kulakova, Ye.V. (2019). *Elektrokataliticheskoe gidrirovanie azotistykh geterotsiklov [Electrocatalytic hydrogenation of nitrogen heterocycles]*. Karaganda: «Glasir» [in Russian].

17 Soboleva, E.A., Visurkhanova, Ya.A., Ivanova, N.M., Beisenbekova, M.E., & Kenzhetaeva, S.O. (2021). Ultrafine copper and nickel powders in the electrocatalytic hydrogenation of organic compounds. *Chem. J. Kazakhstan*, No 2, 32–48. https://doi.org/10.51580/2021-1/2710-1185.26

18 Gawande, M.B. Goswami, A., Felpin, F.-X., Asefa, T., Huang, X., Silva, R, Zou, X., Zboril, R., & Varma R.S. (2016). Cu and Cu-Based Nanoparticles: Synthesis and Applications in Catalysis. *Chem. Rev.*, 116, 3722–3811. https://doi.org/10.1021/acs.chemrev.5b00482

19 Vissurkhanova, Ya.A., Soboleva, E.A., Ivanova, N.M., & Muldakhmetov, Z.M. (2020). Thermal and electrochemical reduction of nickel (II) ferrite under the influence of polymer stabilizers. *Bulletin of the Karaganda University. Chemistry Series*, *98* (2), 42–50. https://doi.org/10.31489/2020ch2/42-50

20 Ivanova, N.M., Soboleva, E.A., Visurkhanova, Ya.A., & Muldakhmetov, Z. (2020). Electrochemical synthesis of Fe–Cu composites based on copper(II) ferrite and their electrocatalytic properties. *Russ. J. Electrochem.*, *56*(7), 533–543. http://doi.org/ HYPERLINK "http://doi.org/10.1134/S1023193520070034"10.1134/S1023193520070034

21 Vasil'ev, V.P., Morozova, R.P., & Kochergina, L.A. (2000*). Praktikum po analiticheskoi khimii [Workshop on analytical chemistry]*. Moscow: Khimiia [in Russian].

22 Olad, A., Alipour, M., & Nosrati, R. (2017). The use of biodegradable polymers for the stabilization of copper nanoparticles synthesized by chemical reduction method. *Bull. Mater. Sci*., *40*(5), 1013-1020. https://doi.org/10.1007/s12034-017-1432-y

23 Maaz, K., Karim, S., Mumtaz, A., Hasanain, S.K., Liu, J., & Duan, J.L. (2009). Synthesis and magnetic characterization of nickel ferrite nanoparticles prepared by co-precipitation. *J. Magn. Magn. Mater*., *321*(12), 1838–1842. https://doi.org/10.1016/j.jmmm.2008.11.098

24 Hu, P., Kang, L., Chang, T., Yang, F., Wang, H., Zhang, Y., Yang, J., Wang, K., Du, J., & Yang, Z. (2017). High saturation magnetization Fe_3O_4 nanoparticles prepared by one-step reduction method in autoclave. *J. Alloy. Compd*., *728*, 88–92. https://doi.org/10.1016/j.jallcom.2017.08.290

25 Inagaki, M. (2009). Pores in carbon materials — importance of their control. *New Carbon Materials*, *24*(3), 193–232. https://doi.org/10.1016/S1872-5805(08)60048-7